JOURNAL OF CATALYSIS **171,** 268–278 (1997)
ARTICLE NO. CA971815

Effect of Zn Content on Catalytic Activity and Physicochemical Properties of Ni-Based Catalysts for Selective Hydrogenation of Acetylene

J. C. Rodríguez,* A. J. Marchi,† A. Borgna,† and A. Monzón*,[1]

*Department of Chemical and Environmental Engineering, University of Zaragoza, 50009 Zaragoza, Spain; and †INCAPE (FIQ, UNL, CONICET), Santiago del Estero 2654, 3000 Santa Fe, Argentina

Received May 9, 1997; revised July 1, 1997; accepted July 1, 1997

The influence of zinc addition on the catalytic performance and physicochemical properties of nickel-based catalysts used in selective hydrogenation of acetylene was investigated. It was found that the activity and selectivity to ethylene of the nickel-based catalysts were positively modified by incorporation of zinc into their solid structure. The zinc-modified catalysts produced smaller amounts of coke and methane than those not containing zinc. Coke deposition had a strong effect on the ethylene selectivity. However, this influence was much more significant for zinc-modified catalysts than for nonmodified nickel-based solids. These results were explained taking into account the different crystalline structures obtained for both types of solid. In the case of zinc-modified catalysts, the metal nickel phase was interacting strongly and highly interdispersed in a nonstoichiometric zinc aluminate spinel matrix. The high interdispersion of the metal nickel phase diminished the number of three-nickel-atom arrangements necessary for the formation of surface intermediates that led to coke and methane production. The nonmodified nickel-based solids, however, were composed of large metal crystallites on which coke and methane precursors were very easily formed. The high interaction between metal nickel particles and the zinc aluminate matrix prevented whisker formation to some extent. Finally, the low concentration of acid sites on the solid surface considerably reduced amorphous-like coke deposition.

1. INTRODUCTION

Ni–Al oxides are commonly used catalysts in reactions such as steam reforming of methane or light hydrocarbons (1, 2), production of synthesis gas (3, 4), and selective hydrogenations (5–7). The high temperature requirements of reforming processes necessitate the use of materials with a good thermal stability (i.e., $NiO–Al_2O_3$). These kinds of material are commonly obtained by decomposition of the binary precipitates at high temperatures, which provides the solid with a spinel-like structure (i.e., $NiAl_2O_4$) (2, 8, 9). The presence of this $NiAl_2O_4$ species is responsible for the thermal stability of the catalyst. Nevertheless, if the decomposition stage is carried out at lower calcination temperatures (i.e., 773–973 K), instead of a normal spinel phase, a metastable phase, commonly called nonstoichiometric or inverse spinel, is obtained. This structure leads to singular catalytic properties (6, 10) as a result of the special coordination sites in which nickel is located. It has been proven that the natural trend of nickel to form large amounts of coke and methane is reduced if inverse $NiAl_2O_4$ species are present in the Ni–Al oxide (4, 7).

As mentioned above, the catalytic activity of the inverse spinel phase seems to be related to the octahedral coordination of Ni^{2+} cations. It has been shown that cations in octahedral holes are preferentially exposed on the surface (5, 6) and that this fact confers singular catalytic properties on solids with spinel-like structures when used in some hydrogenation reactions (6, 7). However, high calcination temperatures (i.e., about 973 K) are necessary to form this spinel phase (3, 4); high reduction temperatures are also required to obtain the active metal nickel phase (3). In addition, the nickel aluminate spinel phase is lost during the reduction process and the final catalyst is constituted by large nickel crystallites in an alumina matrix (3).

It is well known that some other transition metals, such as Zn^{2+}, can also form aluminates with a nonstoichiometric spinel-like structure and that these cations require lower decomposition temperatures than those required by Ni^{2+} spinels to form well-crystallized structures (i.e., 773 K or lower) (5, 11, 12). Furthermore, in some cases, it is possible to preserve the aluminate spinel phase ($ZnAl_2O_4$) after reduction with hydrogen (13, 14). Then, the final catalyst is constituted by a well-dispersed metallic phase in a matrix with a spinel-like structure (15). The attainment of well-dispersed metallic phases can be crucial in the selective hydrogenation of acetylene. Although acetylene hydrogenation is a reaction which is not sensitive to the metallic structure, acetylene hydrogenolisis, a structure sensitive reaction, takes place in parallel to the hydrogenation reactions, giving undesirable products such as coke and methane. Thus, acetylene hydrogenation is in fact a

[1] To whom correspondence should be addressed. Fax: (+34) 976 76 21 42. E-mail: amonzon@posta.unizar.es.

0021-9517/97 $25.00

reaction with an apparent structure sensitivity. Coke and methane are formed from ethylidine species and dissociatively adsorbed acetylene (16–18). The formation of these intermediate species demands a large population of three-atom arrangements. Thus, coke and methane yields can be reduced by physical isolation of the metallic nickel atoms (16). A possibility to reduce the population of the three-atom arrangements could be a solid in which metallic nickel is finely dispersed in a stable spinel-like phase of zinc aluminate.

In this work we have studied the influence of zinc addition on the catalytic performance and physicochemical properties of a Ni-based catalyst with a spinel-like structure, obtained at low calcination temperatures. We also attempt to correlate the catalytic behaviour of these solids in acetylene hydrogenation with their bulk and surface structure.

2. EXPERIMENTAL

The catalysts used in this work were prepared by the coprecipitation method, according to a procedure described elsewhere (12, 13, 15). In order to prepare catalysts, a 1 *M* aqueous solution of the corresponding metallic nitrates and a 1 *M* aqueous solution of K_2CO_3 were simultaneously added into a bidistilled water-containing flask while being stirred vigorously. The pH and temperature of the slurry were kept at 7.2 ± 0.2 and 333 K, respectively, during coprecipitation. The hydrated precursors obtained in this way were separated by filtration, washed with hot bidistilled water, and dried overnight at 453 K. The corresponding mixed oxides were obtained by treating the dried hydrate precursors in N_2 at 773 K for 14 h. The composition and specific area of the mixed oxides used in this work are shown in Table 1.

The specific surface area of the different mixed oxides was measured by adsorption of N_2 at 77 K with a Micromeritis Pulse Chemisorb 2700 using the multipoint technique. The bulk composition of the mixed oxides was determined by ICP–AES (inductively coupled plasma–atomic emission spectrometry) in a Yobin–Ivon J424 spectrometer. The XRD (X-ray diffraction) patterns have been obtained within the range of 5 to 80° (2θ) operating at a scanning rate of 0.2 (2θ)/s in a Rygaku/Max system diffractometer. A graphite monochromator was used with the aim of selecting the Cu$K\alpha$ radiation ($\lambda = 1.5418$ Å). The TPR (temperature programmed reduction) experiments were carried out in a flow system equipped with a TCD (thermal conductivity detector) and PCLD-889 and PCL-812PG cards for data acquisition. The experimental profiles were obtained by using a H_2 6%/N_2 mixture and 200 mg of sample. The heating rate was 10 K/min and a maximum temperature of 1173 K was reached in all cases. The XPS (X-ray photoelectron spectroscopy) spectra were recorded with a Surface Science Instrument (SSI) spectrometer, using Al$K\alpha$ radiation. The C1*s* band at 284.9 eV was used as an internal standard. The system is equipped with an *in situ* chamber in which pretreatment of samples was carried out before analysis. Pyridine adsorption was used to determine the kind of acid sites and the total acidity of the samples. FTIR (Fourier transform infrared spectroscopy) spectra were recorded with a Nicolet 740 instrument. SEM (scanning electron microscopy) micrographs of catalysts, before and after reaction, were obtained with a JEOL JSM 6400 microscope. The solids were covered by electrodeposition with a thin gold film to improve sample conductivity.

Acetylene hydrogenation was performed in gas phase by using a thermogravimetric system (CI Electronics Ltd., model MK2) equipped with mass flow and temperature controllers. The thermogravimetric system was coupled to a PC provided with a CI Electronics Multicard for data acquisition, which allows continuous registering of the sample weight changes and temperature during reaction. Catalyst activation (reduction) was carried out *in situ* at 773 K for 2.5 h using H_2 (vol. 50%)/N_2 mixture with a total flowrate of 100 Nml/min. This activation temperature was selected to minimise the sintering of the Ni crystallites (19). After activation, a $H_2/C_2H_2/N_2$ mixture (composition: 60/15/25) and a total flow rate of 700 Nml/min was fed to the thermogravimetric system while the temperature was kept at 448 K. In all cases, the amount of catalyst used was 200 mg. The analysis of the product stream and unconverted reactant was performed with a Hewlett–Packard 5890 II chromatograph equipped with a Carboxen 100 packed column and FID (flame ionization detector).

TABLE 1

Summary of the Different Mixed Oxides Prepared. Nominal Composition and BET Surface Areas

Sample	Nominal composition	M^{2+}/M^{3+}	Ni/Al	Zn/Al	Sg (m^2/g)
Ni(0.5)/Al	$(NiO)_{0.5}Al_2O_3$	0.5	0.5	0	255
Ni/Al	$(NiO)Al_2O_3$	1.0	1.0	0	235
Ni(0.5)/Zn/Al	$(NiO)_{0.5}(ZnO)_{0.5}Al_2O_3$	1.0	0.5	0.5	210
Ni(0.25)/Zn/Al	$(NiO)_{0.25}(ZnO)_{0.75}Al_2O_3$	1.0	0.25	0.75	205
Zn/Al	$(ZnO)Al_2O_3$	0.5	0	0.5	121

Note. M^{2+}/M^{3+}: atomic ratio between dipositive and tripositive cations. M^{2+}: Ni and Zn; M^{3+}: Al.

3. RESULTS

3.1. Characterization

The XRD patterns of the dried precipitates are shown in Fig. 1. Two poorly defined phases were detected in the Ni–Al samples: aluminium hydroxide (ASTM 7-324) and hydrotalcite-like (ASTM 14-191). The degree of

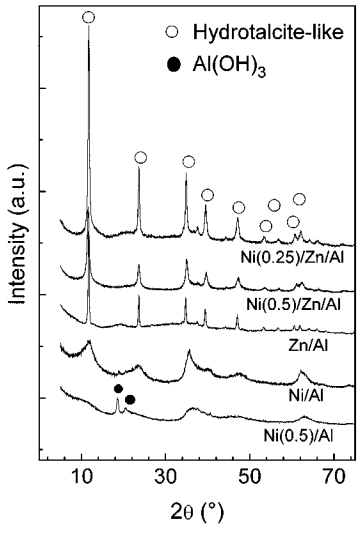

FIG. 1. XRD patterns of hydrated precursors obtained by coprecipitation at pH constant.

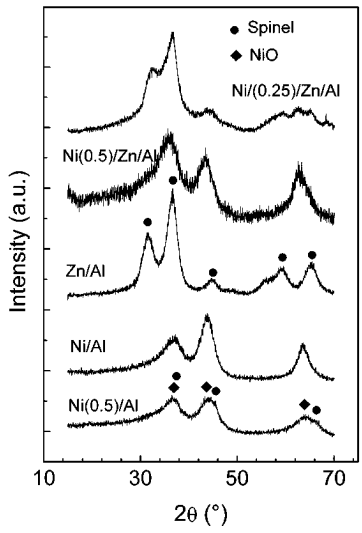

FIG. 2. XRD patterns of mixed oxides obtained by thermal treatment in N_2 at 773 K.

crystallinity of these samples is noticeably low, indicating that the main component is an amorphous phase. This means that only heterogeneous precursors can be obtained by coprecipitation of Ni^{2+} and Al^{3+} cations when K_2CO_3 is used as a precipitant reagent and working at a pH approximately equal to 7.0. In contrast, only a well-crystallized hydrotalcite-like phase was observed for the case of zinc-containing hydrated precursors. Furthermore, it is easy to observe that their degree of crystallinity is higher than that obtained in the Ni–Al samples, especially in the Ni(0.25)/Zn/Al sample. These results indicate that it is possible to obtain coprecipitates of high homogeneity at a pH equal to 7.0 when zinc is part of the solid structure.

The XRD patterns of the corresponding mixed oxides are shown in Fig. 2. Two phases were detected in the binary Ni/Al mixed oxides: a spinel-like phase, probably nickel aluminate, and nickel oxide. The most intense signal for a nickel aluminate of spinel-like structure is at $2\theta = 37.1^\circ$ (ASTM 10-339) while for nickel oxide it is at $2\theta = 43.4^\circ$ (ASTM 22-1189). It is found that the I_{37}/I_{43} ratio grows as the nickel content decreases. This indicates that, in binary Ni/Al solids, the amount of $NiAl_2O_4$ with respect to NiO becomes more important as the nickel load is reduced. The addition of Zn leads to a further increase of the I_{37}/I_{43} ratio. Thus the peak at $2\theta = 43.4^\circ$ almost disappears in the sample Ni(0.25)/Zn/Al and its XRD pattern fully resembles that of the binary Zn/Al sample. The XRD pattern of the binary Zn/Al oxide is in good agreement with that of a zinc aluminate spinel (ASTM 5-0669). These results allow us to conclude that the content of spinel-like phase in the series of mixed oxides increases in the following order: Ni/Al < Ni(0.5)/Al < Ni(0.5)/Zn/Al < Ni(0.25)/Zn/Al < Zn/Al.

The specific surface area of the different samples followed just the opposite order (see Table 1). Therefore, binary Zn/Al oxide has the lowest area (i.e., 120 m^2/g). This is in agreement with the fact that this solid has the highest crystallite size and degree of crystallinity. All samples containing Ni exhibit areas between 200 and 250 m^2/g.

According to the TPR profiles, Ni reducibility is almost the same in all the mixed oxides used in this work (see Fig. 3). In addition, the reducibility of Ni spinel-like phases is considerably lower than that found for pure NiO (20). In the case of pure NiO, the maximum H_2 consumption is reached at around 673 K. However, for the samples prepared in this work the reduction starts between 673 and 723 K, reaching a maximum H_2 consumption at around 893 K. The nickel content calculated by means of

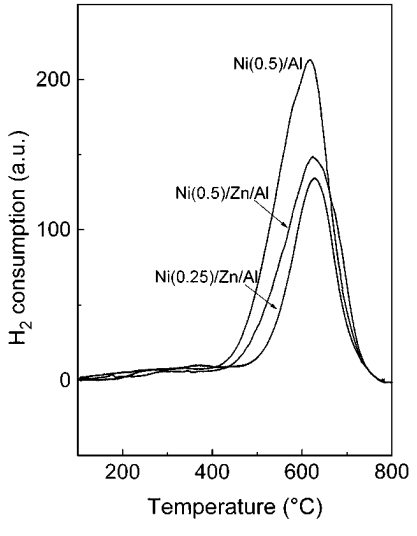

FIG. 3. TPR profiles of mixed oxides obtained by thermal treatment in N_2 at 773 K.

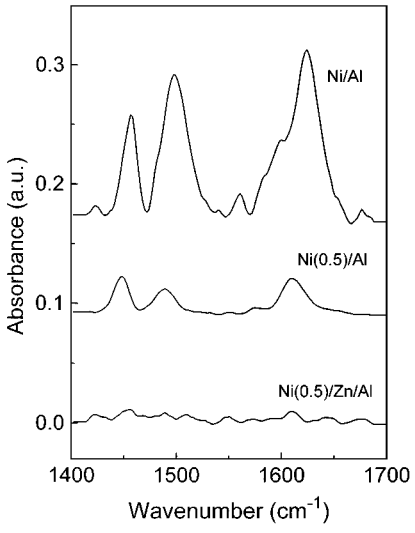

FIG. 4. FTIR of adsorbed pyridine on mixed oxides obtained by thermal treatment in N_2 at 773 K.

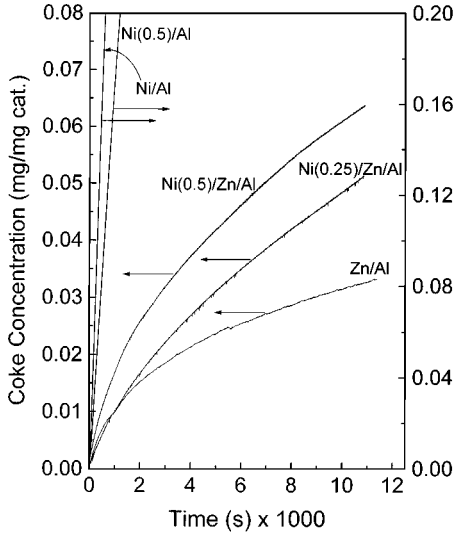

FIG. 5. Coke profiles during acetylene hydrogenation on activated nickel-based catalysts.

the hydrogen uptake obtained from TPR data was in a good agreement with the values determined by ICP-AES (Table 1 and Fig. 3).

FTIR spectra after pyridine adsorption revealed that both Lewis and Brønsted acid sites were present on the surface of mixed oxides (see Fig. 4). The bands at around 1595, 1575, 1490–1500, and 1450–1460 cm^{-1} are normally assigned to pyridine adsorbed on Lewis acid sites, while bands at around 1650, 1630, 1550, and 1490 cm^{-1} are usually related to pyridine adsorbed on Brønsted acid sites (21). The concentration of acid sites decreases as the nickel content diminishes. Further, Zn addition leads to a great reduction of the amount of acid sites on the mixed oxide surface. Thus, only some evidence of Lewis sites was found in the zinc-containing oxides.

Both calcined and reduced samples were analyzed by XPS. The reduction process was carried out *in situ*, in H_2 atmosphere at 773 K for 2.5 h. The results obtained by XPS are summarized in Table 2. It can be observed that after reduction only between 40 and 50% of nickel on the surface was metallic, the rest remaining as Ni^{2+}. It is also interesting to note that the amount of metallic nickel is somewhat lower in the case of Zn-containing samples. No significant differences in the binding energy of the different cations were observed from the comparison of binary and ternary oxides. Furthermore, no evidence of Zn or Al reduction was detected. Finally, the values of atomic ratios indicate that: (a) the surface is poorer in Ni and Zn than the bulk and (b) the surface becomes poorer in Ni after the reduction treatment, which indicates some degree of Ni sintering.

3.2. *Catalytic Activity*

The weight increase of the catalyst sample was continuously monitored during reaction. This increment was mainly due to the adsorption of coke precursors and their further transformation into coke. As is shown in Fig. 5, the amount of coke deposited on the binary Ni/Al catalysts

TABLE 2

XPS Results before and after Reduction Treatment

Elements, oxidation states and atomic ratios	Ni/Al						Ni/Zn/Al					
	B.E. (eV)		%		Atomic ratios		B.E. (eV)		%		Atomic ratios	
	Calc.	Red.	Calc.	Red.	Calc.	Red.	Calc.	Red.	Calc.	Red.	Calc.	Red.
Ni^{2+}	856.5	856.3	100	45			856.2	856.5	100	60		
Ni^0	—	852.8	—	55			—	853.0	—	40		
Zn^{2+}	—	—	—	—			1022.5	1022.5	100	100		
Al^{3+}	74.4	74.4	100	100			74.4	74.4	100	100		
Ni/Al					0.07	0.06					0.13	0.10
Zn/Al					0	0					0.13	0.17
Ni/Zn					0	0					1	0.58

Note. Calc. = calcined sample; Red. = sample reduced at 773 K during 2.5 h.

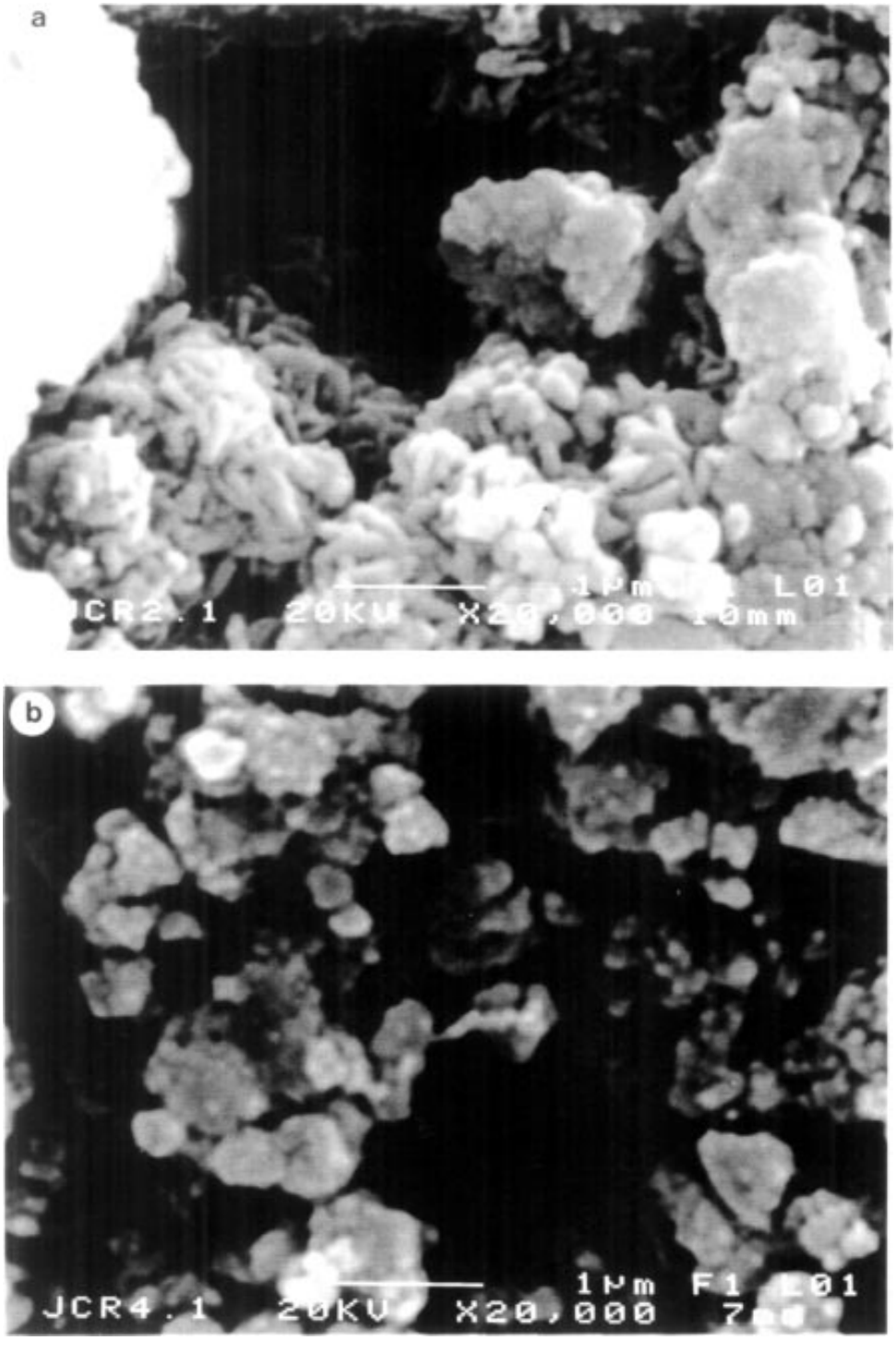

FIG. 6. SEM micrographs of binary and ternary catalysts after exposure to reactant stream: (a) Ni/Al sample after 5 min of reaction; (b) Ni/Al sample after 3 h of reaction; (c) Ni(0.5)/Zn/Al after 5 min of reaction; (d) Ni(0.5)/Zn/Al after 3 h of reaction.

increased dramatically with time. Thus, the amount of coke deposited on these samples after only 15–20 min of reaction was around 20 wt.%. In contrast, coke deposition was much less important in ternary Ni/Zn/Al catalysts. The quantity of coke formed over these samples was less than 7 wt.% after almost 3 h of reaction. The lowest amount of coke was observed for the $ZnAl_2O_4$ sample. These results indicate that coke formation and the initial coking rate diminish as the Ni/Zn ratio is decreased, which means that nickel is also responsible for coke formation. Furthermore, zinc inclusion

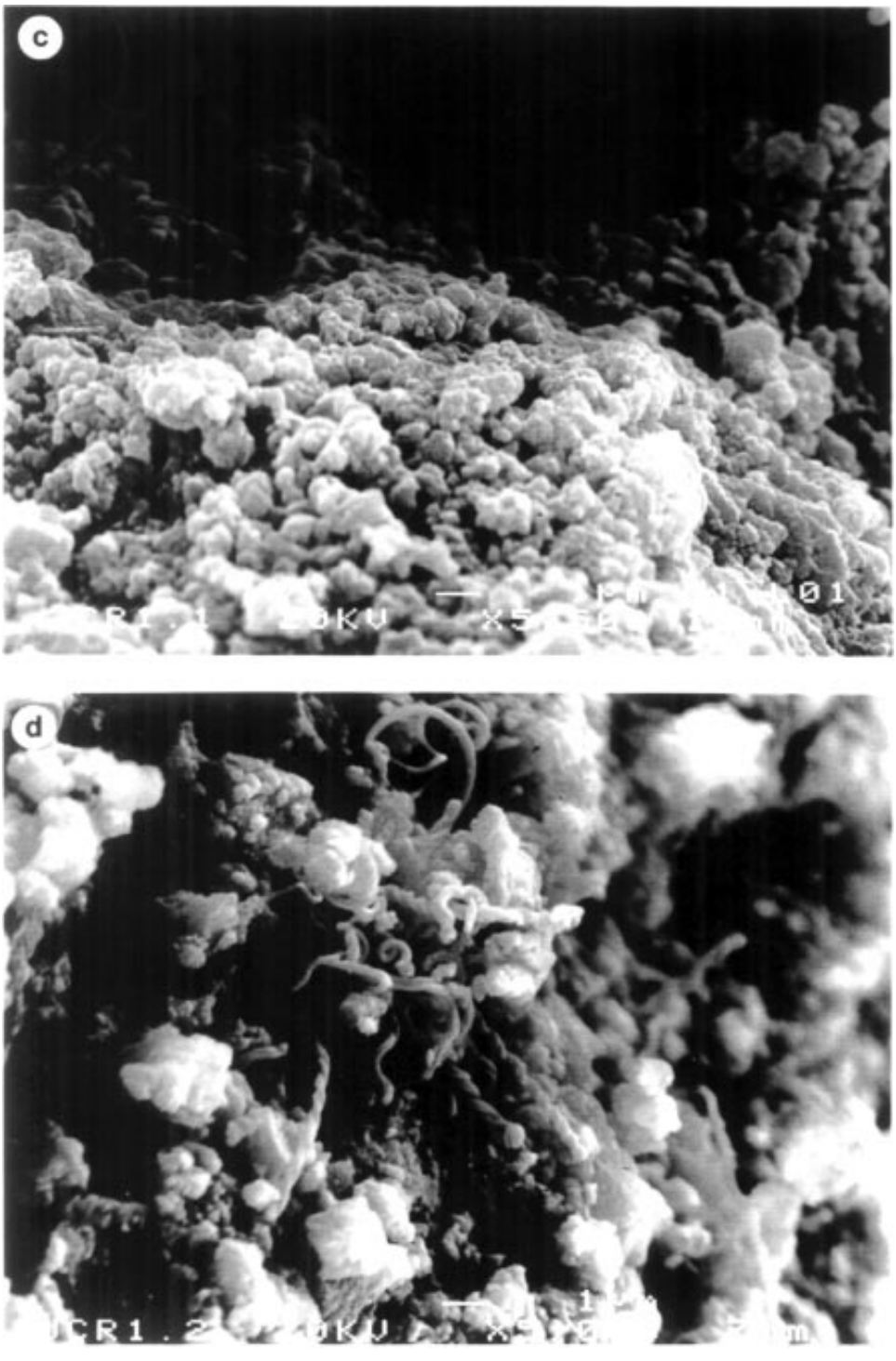

FIG. 6—*Continued*

into the matrix structure seems to reduce coke deposition considerably.

Catalysts were observed by SEM after reaction. From the analysis of the micrographs it can be concluded that at least two types of coke are formed on Ni-based catalysts during acetylene hydrogenation: (a) whiskers and (b) amorphous-like coke. In the case of binary Ni/Al catalysts, whiskers are easily formed at the first stages of reaction (see Fig. 6a). At the end of the run, the large amount of amorphous-like coke deposited on these samples occluded the whiskers

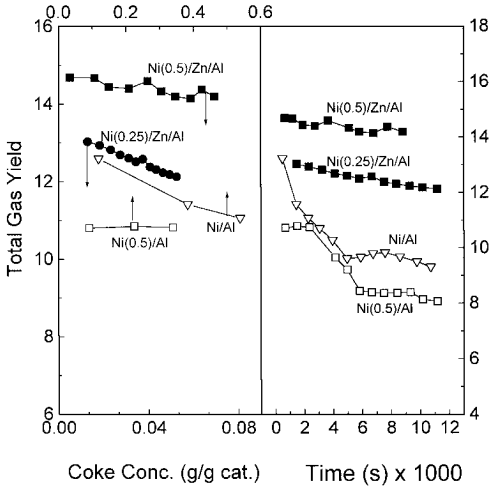

FIG. 7. Total gas yield (g of gas products/100 g of C_2H_2 fed) vs coke concentration on catalyst surface and time.

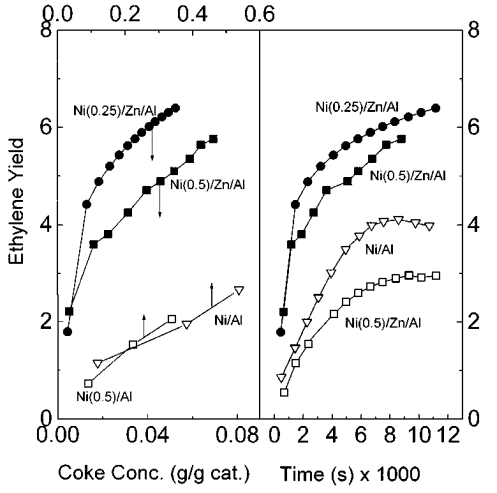

FIG. 8. Ethylene yield (g of C_2H_4/100 g of C_2H_2 fed) vs coke concentration and time.

formed in the first reaction stage (Fig. 6b). However, in ternary samples, no whisker generation was observed at the beginning of reaction (Fig. 6c) but whiskers were the main coke species detected on this type of solids at the end of the run (Fig. 6d). These SEM photographs, obtained at different reaction times, fully agree with the fact that the total coke deposition and the initial coking rate, determined with the help of the thermogravimetric system, are lower in the case of ternary Ni/Zn/Al catalysts.

The catalytic activity of clean Ni-based catalysts depends on the nickel content (Fig. 7a). In the case of ternary Ni/Zn/Al samples, the total yield at a zero coke content was 12 and 8 g total products per 100 g C_2H_2 fed for Ni(0.5)/Zn/Al and Ni(0.25)/Zn/Al, respectively. For binary Ni/Al samples, the corresponding values were 14 and 11 g total products/100 g of C_2H_2 fed for Ni(0.5)/Al and Ni/Al, respectively. This means that even when the nickel content is higher in the binary solids, the intrinsic activity of ternary catalysts is somewhat higher than that corresponding to binary catalysts. Besides, as the coke content rose, the total yield increased in the case of ternary Ni/Zn/Al catalysts until an approximately constant value (Figs. 7a and 7b). Coke deposition had the opposite effect on binary Ni/Al catalysts, since the total yield diminished during coke deposition until reaching a quasi-steady state (Fig. 7b). The final total yields were somewhat higher in ternary catalysts than in the binaries (Figs. 7a and 7b). Thus, coke deposition had a "beneficial" effect on the catalytic activity of ternary samples and a negative effect in the activity of the binary solids. The most pronounced effect of coke was observed for the ternary sample with the lowest nickel content. Finally, it must be remarked that the $ZnAl_2O_4$ sample, after the reduction treatment, did not show any activity for acetylene hydrogenation, and only a small activity for coking.

Regarding the distribution of the reaction products in the outlet stream, the initial ethylene yield was almost zero in all the cases (Fig. 8). Nevertheless, the ethylene yield increased in parallel with coke deposition until an approximately constant was value reached. The effect of coke on ethylene yield was by far more important in the ternary Ni/Zn/Al catalysts than in binary samples (Fig. 8a). Furthermore, the influence of coke seemed to be more important as the Ni/Zn ratio decreased. Thus, the maximum ethylene yield and selectivity were found in the Ni(0.25)/Zn/Al catalyst. In contrast, with binary Ni/Al solids, ethylene yields of 3–4% were only attained after a long period of contact (Fig. 8b), corresponding to coke concentrations much higher than 60%.

In all cases, the initial methane yield was not zero. The values depended on the type of catalyst and its nickel content (Fig. 9). Methane yields were much higher in binary

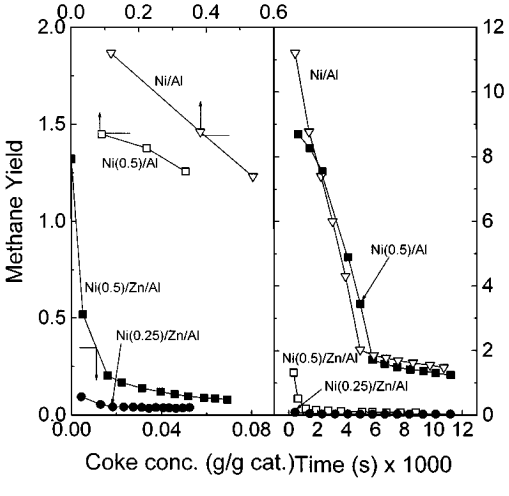

FIG. 9. Methane yield (g of CH_4/100 g of C_2H_2 fed) vs coke concentration and time.

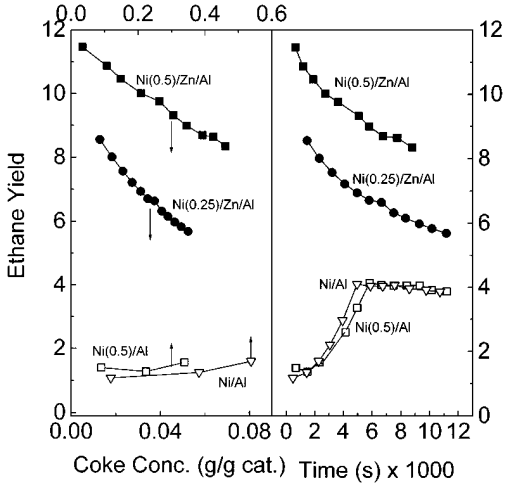

FIG. 10. Ethane yield (g of C_2H_6/100 g of C_2H_2 fed) vs coke concentration and time.

Ni/Al catalysts than in ternary Ni/Zn/Al. Besides, for a given series of catalyst (i.e., binaries or ternaries), the initial methane yield diminished as the nickel content in the solid was lower. This is the opposite behaviour to that observed for the ethylene yield. In addition, the methane yield decreased with coke deposition (Figs. 9a and 9b). In the case of binary Ni/Al solids, methane is the main product in the gas phase during the first stage of reaction and even during the last stage of reaction. Nevertheless, in Ni/Zn/Al samples, the methane yield dropped rather fast to zero. Finally, it must be pointed out that in Ni/Al catalysts, the evolution of the methane yield over time is similar to that observed for the total yield (see Figs. 7 and 9).

Ni/Zn/Al catalysts gave an initial ethane yield higher than Ni/Al samples (Fig. 10). The evolution of the ethane yield over time was different for samples containing Zn with respect to those based only in Ni and Al. Thus, in the case of ternary samples, the ethane yield reached a maximum for a coke concentration lower than 2% and then decreased slowly with coke deposition. This evolution is similar to that observed for the total yield (Figs. 7 and 10). In the case of Ni/Al solids, the ethane yield increased quite fast to an almost constant value (Fig. 10b). This evolution is just the opposite to that observed for the total and methane yields (Figs. 7, 9, and 10). The evolution of the ethane yield over time was almost the same in both Ni/Al catalysts (Fig. 10b). However, in the case of ternary catalysts, the ethane yield was always lower for Ni(0.25)/Zn/Al than for Ni(0.5)/Zn/Al (Fig. 10).

4. DISCUSSION

In this work, it has been shown that the catalytic behaviour of nickel-based catalysts in the selective hydrogenation of acetylene changes dramatically when zinc is added to the solid structure. The main influence of zinc addition is an important diminution of methane yield and coke deposition, both being undesirable products of this reaction. Coke deposition is shown to produce a positive effect on ethylene selectivity and yield in both binary and ternary catalysts. However, this "beneficial" effect is more remarked for ternary Ni/Zn/Al catalysts even when the amount of coke deposited on the surface of these solids is smaller than in Ni/Al samples. The negative effect of coke on the catalyst stability (decrease of the conversion level over reaction time) seems to be the case of somewhat more pronounced binary Ni/Al catalysts. Finally, ethane selectivity and yield diminishes in parallel to coke deposition on Ni/Zn/Al solids, while the opposite is true for binary Ni/Al solids.

These results can be explained on the basis of the mechanisms suggested by Somorjai (22) and Margitfalvi *et al.* (23). A general scheme that summarizes the idea suggested by these authors is shown in Fig. 11. According to this mechanism, three different types of hydrocarbon intermediate can be formed on the metal surface: 1) adsorbed acetylene, which by further hydrogenation would give ethylene, which is the desired product; 2) strongly adsorbed ethylidine species, which by further hydrogenation produce ethane; 3) acetylene dissociatively adsorbed, which is a coke precursor. Coke production from this acetylene species involves a two step process: 1) hydrogenolisis of adsorbed species to give methylene adsorbed species; 2) migration of the adsorbed methylene under the metal particles to form whiskers. If some of the species formed by hydrogenolisis interact with chemisorbed hydrogen, then methane is produced. Hydrogenations of hydrocarbons are known to be structure insensitive reactions. However, according to the mechanism in Fig. 11, any factor that serves to reduce the number of three-atom-arrangements will contribute to a lower methane yield, coke production and probably ethane yield. Thus, acetylene hydrogenation has an apparent structure sensitivity (24). Den Hartog *et al.* (25)

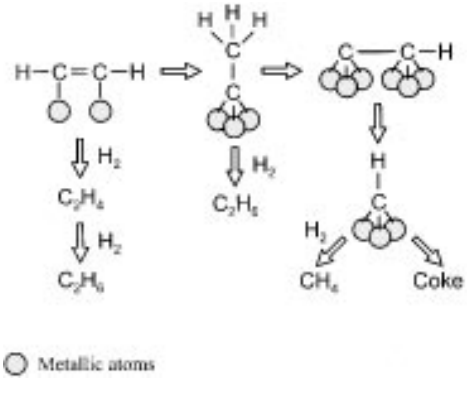

FIG. 11. General scheme of overall proposed mechanism for acetylene hydrogenation.

studied the alloying of Pt, Pd, Ir, and Rh catalysts and the influence of the metallic particle size on the ethylene selectivity. They found that the concentration of ethylidine species diminishes when the number of neighbour active atoms was also decreased by alloy formation. Thus, ethane selectivity could be diminished and ethylene selectivity increased. A similar effect was observed in a study carried out with Pt/SiO_2 catalysts partially deactivated by chlorine (26).

On the basis of the previous discussion, the lower coke deposition and methane yield observed for ternary Ni/Zn/Al catalysts with respect to the binary Ni/Al ones can be explained. According to the XRD patterns, NiO is more interdispersed in the zinc aluminate spinel-like matrix than in the alumina-like matrix. Thus, it is assumed that the metallic nickel particles, obtained after reduction in H_2, are smaller and the interaction of these particles with the matrix is stronger in Ni/Zn/Al catalysts than in Ni/Al solids. This difference in the metal-support interaction can potentially alter the electronic state of nickel. However, neither TPR nor XPS revealed the existence of any important electronic effect. The TPR experiments did not reveal any significant differences between binary and ternary samples concerning nickel reducibility. In addition, the XPS results showed a similar binding energy for Ni^0 in both types of sample. Thus, the differences in catalytic performance are not due to an electronic effect. The reason is more likely to be a reduction of the number of neighbour nickel atoms, which would lead to a diminution of three-atom-arrangements. The smaller the number of three-atom-sites, the lower the concentration of coke precursors, i.e. of dissociatively adsorbed acetylene (Fig. 1). However, the reduction of three-atom-arrangements in Ni/Zn/Al catalysts was not enough to avoid ethane production and, in fact, this was the main product at the beginning of the reaction. It is important to remark that a maximum in the ethane and total yields was obtained (ca. 2% coke content). This maximum very likely is caused by the transient period during which acetylene is dissociatively and strongly adsorbed on the surface, poisoning part of the three-atom-sites and causing a decrease in methane and coke yields. In Ni/Al solids, the metal nickel particles are large enough to have a large population of three-atom-arrangements, and therefore to produce a high concentration of dissociatively adsorbed acetylene which initially leads to large amounts of methane and coke precursors. In this case, the yield to these undesirable products decreases slowly along with coke deposition, in agreement with the two facts mentioned above: 1) the existence of large metal particles; 2) the deposition of amorphous coke that does not cause the separation of metal particles from the surface by whisker formation.

There is still another possibility to explain the different catalytic behaviour of binary and ternary nickel-based catalysts. Taking into account the different nature of the matrix and the different crystallite size of the metallic nickel particles, it is very likely that the exposed crystalline planes of metallic particles are different for binary and ternary catalysts. It is well known that the adsorption strength depends on the plane on which molecules interact. The closer the structure, the lower the adsorption strength. Thus, dissociative acetylene adsorption, and therefore methane and coke production, should be disfavoured in surfaces exposing planes with a closer structure. This could be the case with Ni/Zn/Al catalysts, and the opposite being the with Ni/Al.

Coke plays an important role in the selective hydrogenation of acetylene. The methane yield decreases and the ethylene yield increases as coke is formed on the surface of both binary and ternary catalysts. Part of the coke precursors, probably remains on the metallic surface as dissociatively adsorbed acetylene, poisoning the three-atom-arrangements. The diminution of the number of these sites leads to a lower methane yield, as shown in Fig. 11. In contrast, acetylene hydrogenation into ethylene is a facile reaction that can be carried out even on the ethylidine species layer (22). Thus, as the number of neighbour nickel atoms decreases, acetylene hydrogenation becomes favoured against hydrogenolisis, this effect being faster and more pronounced in the case of ternary Ni/Zn/Al catalysts than with Ni/Al, due to the larger crystallite size of the latter. The weaker interaction of nickel particles with the alumina matrix also allows whiskers to be more easily formed at the start of the reaction.

The ethane yield increased with coke content for Ni/Al catalysts while for Ni/Zn/Al catalysts the trend was the opposite. This means that the diminution of the number of three-atom-arrangements in ternary catalysts, due to coke deposition, is enough to reduce the ethane yield. However, while the methane yield dropped very fast to almost zero, the ethane yield decreased to a quasi-steady-state above zero. Thus, it could be suggested that hydrogenolisis (a very structure sensitive reaction) is much more affected by the reduction of the number of neighbour nickel atoms than is ethane production. The contrary effect was obtained with Ni–Al catalysts, i.e. the ethane yield increased over time until a quasi-steady-state was reached. In this case, because of the large size of the metallic arrangements, the coke deposition enhances ethane production, (which requires smaller metallic ensembles than methane formation), rather than ethylene production, the least sensitive reaction of the three. This behaviour is in agreement with the fact that ethane can be produced on two different types of site (7, 27), as shown in Fig. 11. According to the results found by Guczi *et al.* (28) and Margitfalvi *et al.* (23), it can be suggested that ethane is produced from both ethylidine species and direct hydrogenation of acetylene. As coke deposition increases the number of neighbour nickel atoms is reduced and, therefore, ethane production

from direct acetylene hydrogenation becomes more significant.

One of the most important differences between ternary and binary samples is the amount and type of coke formed. Whiskers seem to be more easily formed at the first stages of reaction on binary Ni/Al solids, as was detected by SEM. Mechanisms for whisker formation have already been suggested by several authors (18, 29, 30). These mechanisms have been used to explain the non-deactivating effect of this type of coke. The limiting step in whisker generation seems to be carbon diffusion under the nickel particle, which would lead to a high activation energy for the overall process. Usually values in the range 20–35 kcal/mol (18, 29, 30) have been reported for the activation energies of carbon diffusion through metallic crystallites. It could be supposed that carbon diffusion and, as a consequence, whisker growth is made more difficult when the interaction between metallic particles and the support becomes more significant. This is in agreement with the different interaction of metallic nickel particles with zinc aluminate and alumina matrix, as suggested above. This can explain the faster whisker formation on binary Ni/Al catalysts at the first stages of reaction. After exposing the catalyst to the reactant atmosphere for some time (i.e., 3 h), coke concentration was higher by far on Ni/Al catalysts than on Ni/Zn/Al catalysts. In addition, coke deposited on binary solids had an amorphous appearance. The formation of this amorphous coke can be associated with the high concentration of acid sites observed on the surface of the binary samples. Lewis and Brønsted sites were almost absent on the surface of the zinc aluminate phase, in agreement with the fact that no amorphous coke was observed on ternary Ni/Zn/Al catalysts, even after a long exposure time to the reactant mixture.

5. CONCLUSIONS

The activity and selectivity of Ni-based catalysts, used in the selective hydrogenation of acetylene, can be improved by incorporating Zn^{2+} in the solid structure. The zinc-modified catalysts produce smaller amounts of coke and methane in comparison with those not containing zinc. Furthermore, coke deposited on ternary Ni/Zn/Al catalysts has a strong effect on ethylene production.

The reason for the different catalytic behaviour could be the different crystalline structure obtained when zinc is present in the catalyst matrix. Zinc addition favours the formation of non-stoichiometric spinel-like phases, even at low calcination temperatures. These spinel phases are quite stable in the reaction conditions used in this work. The result is a solid in which Ni^{2+} cations are highly interdispersed in the zinc aluminate phase. The activation process by reduction with hydrogen leads to solids in which the metallic nickel particles are strongly interacting with the zinc aluminate matrix. Their high dispersion reduces the concentration of neighbour nickel atoms and thus also methane and coke yields. The high interaction between metallic particles and zinc aluminate to some extent prevents formation. Finally, the low concentration of acid sites on the solid surface considerably reduce amorphous-like coke deposition.

ACKNOWLEDGMENTS

The authors gratefully acknowledge the financial support of DGYCIT (Spain) for this work (Project PB94-0568). We also acknowledge the help of Professor A. T. Aguayo (Bilbao, Spain), who carried out the FTIR measurements.

REFERENCES

1. Al-Ubaid, A., and Wolf, E. E., *Appl. Catal.* **40**, 73 (1988).
2. Ross, J. R. H., Steel, M. C. F., and Zeini-Isfahani, A., *Appl. Catal.* **52**, 280 (1978).
3. Bhattacharyya, A., and Chang, V. W., *in* "Catalysts Deactivation 1994" (B. Delmon and G. F. Froment, Eds.), Vol. 88, p. 207. Elsevier, Amsterdam, 1994.
4. Chen, Y. G., and Ren, J., *Catal. Lett.* **29**, 39 (1994).
5. Cavani, F., Trifiró, F., and Vaccari, A., *Catal. Today* **11**, 173 (1991).
6. Jacobs, J. P., Maltha, A., Reintjes, J. G. H., Drimal, J., Ponec, V., and Brongersma, H. H., *J. Catal.* **147**, 294 (1994).
7. Peña, J. A., Herguido, J., Guimon, C., Monzón, A., and Santamaría, J., *J. Catal.* **159**, 313 (1996).
8. Trifiro, F., Vaccari, A., and Clause, O., *Catal. Today* **21**, 185 (1994).
9. Clause, O., Rebours, B., Merlen, E., Trifiro, F., and Vaccari, A., *J. Catal.* **133**, 231 (1992).
10. Trifiro, F., and Vaccari, A., *in* "Structure-Activity and Selectivity Relationship in Heterogeneous Catalysis" (R. K. Graselli and A. W. Sleight, Eds.), p. 157. Elsevier, Amsterdam, 1991.
11. Courty, Ph., Durand, D., Freund, E., and Sugier, A., *J. Mol. Catal.* **17**, 241 (1982).
12. Marchi, A. J., Di Cosimo, J. I., and Apesteguía, C. R., *in* "Proceedings, 10th International Congress on Catalysis, Budapest, 1992" (L. Guczi, F. Solymosi, and P. Tetenyi, Eds.), p. 1771. Akadémiai Kiadó, Budapest, 1993.
13. Marchi, A. J., Di Cosimo, J. I., and Apesteguía, C. R., *Catal. Today* **15**, 383 (1992).
14. Grandvallet, P., Courthy, Ph., and Freund, E., *in* "Proceedings, 8th International Congress on Catalysis, Berlin, 1984," Vol. II, p. 81. Dechema, Frankfurt-am-Main, 1984.
15. Marchi, A. J., Di Cosimo, J. I., and Apesteguía, C. R., *in* "Proceedings, 9th International Congress on Catalysis, Calgary, 1988" (M. J. Phillips and M. Ternan, Eds.), Vol. II, p. 529, Chem. Institute of Canada, Ottawa, 1988.
16. Moses, J. H., Weiss, A. H., Matusek, K., and Guczi, L., *J. Catal.* **86**, 417 (1984).
17. Somorjai, G. A., Kesmodel, L. L., and Dubois, L. H., *J. Chem. Phys.* **20**, 2180 (1979).
18. Lobo, L. S., Trimm, D. L., and Figuereido, J. L., *in* "Proceedings, 5th International Congress on Catalysis, Palm Beach, 1972" (J. W. Hightower, Ed.), p. 1125. North-Holland, Amsterdam, 1973.
19. Peña, J. A., Rodriguez, J. C., Herguido, J., Santamaría, J., and Monzón, A., *in* "Catalyst Deactivation 1994" (B. Delmon and G. F. Froment, Eds.), Stud. Surf. Sci. and Catal., Vol. 88, p. 555. Elsevier, Amsterdam, 1994.

20. Bolt, P. H., Habraken, F. H. P. M., and Geus, J. W., *J. Catal.* **151**, 300 (1995).
21. Jacobs, P. A., *in* "Characterization of Heterogeneous Catalysts" (F. Delannay Ed.), Chap. 8, p. 381. Dekker, New York, 1987.
22. Somorjai, G. A., *in* "Catalysis Design Progress and Perspectives" (L. L. Hegedus Ed.). Wiley, New York, 1987.
23. Margitfalvi, J., Guczi, L., and Weiss, A. H., *J. Catal.* **72**, 195 (1981).
24. Dorling, T. A., and Hoss, R. L., *J. Catal.* **7**, 378 (1967).
25. Den Hartog, A. J., Deng, M., Jongerius, F., and Ponec, V., *J. Mol. Catal.* **60**, 99 (1990).
26. Butt, J. B., and Petersen, E. E., *in* "Activation, Deactivation and Poisoning of Catalysts." Academic Press, San Diego, 1988.
27. McGown, W. T., Kemball, C., Whan, D. A., and Scurrell, M. S., *J. Chem. Soc. Faraday Trans. I* **73**, 632 (1977).
28. Guczi, L., La Pierre, R. B., Weiss, R. B., and Bell, W. K., *J. Catal.* **60**, 83 (1979).
29. Trimm, D. L., *Catal. Rev. Sci. Eng.* **16**, 155 (1977).
30. Figuereido, J. L., *in* "Proceedings of the NATO Advanced Study Institute on Catalysis Deactivation" (J. L. Figueiredo, Ed.), p. 45. Kluwer Academic, Algarve, 1981.